

Research Article

Microfacies and Reservoir Space Characteristics of Carbonate Reservoir of the Ordovician Yingshan Formation in Northern Slope of Tazhong Uplift, Tarim Basin

Ping Ren ^{1,2}

¹PetroChina Research Center of Salt-Cavern UGS Technology, China

²PetroChina Gas Storage Company, China

Correspondence should be addressed to Ping Ren; renp-tlm@petrochina.com.cn

Received 6 October 2022; Revised 7 November 2022; Accepted 24 November 2022; Published 15 February 2023

Academic Editor: Zhongwei Wu

Copyright © 2023 Ping Ren. This is an open access article distributed under the Creative Commons Attribution License, which permits unrestricted use, distribution, and reproduction in any medium, provided the original work is properly cited.

As an important stratum of exploration in the Tarim Basin, which is the largest petroleum basin in China, Yingshan Formation has great potential. The relationship between the fine division of microfacies and reservoir space characteristics has not been systematically studied which restricts further exploration. On the basis of the analysis of core, thin section, logging data, imaging logging data (FMI), and field outcrop, the microfacies types and reservoir space characteristics of the Ordovician Yingshan Formation are systemically studied. The results show that (1) nine microfacies (Mf1-Mf9) and four microfacies associations (MA1-MA4) were identified within the Ordovician Yingshan Formation. MA1-MA2 represent a medium- to high-energy sedimentary background, and MA3-MA4 represent a medium- to low-energy sedimentary background. (2) Four reservoir space types were observed in the Yingshan Formation, which are dominated by fracture-dissolution pore type, followed by small dissolution vug type, seldom fracture type, and large-scale karst-cavity type. (3) High-energy microfacies are the material basis of favorable reservoirs. The high-energy microfacies associations are prone to small dissolution vug and fracture-dissolution pore types of reservoirs; large cave reservoirs can sometimes be developed in the high part of the sequence and form favorable reservoirs in the Yingshan Formation. The low-energy microfacies associations mostly appear as original strata or interlayer, but after the superposition of structural cracks, buried karsts, or epigenetic karsts, low-energy microfacies associations may form relatively small-scale fractured and fracture-dissolution pore types of reservoirs in this area.

1. Introduction

Carbonate rock can form a variety of different types of reservoir space, which is an important place and channel for oil and gas preservation and flow [1]. The microfacies of carbonate rocks are the material basis for the spatial development of different types of reservoirs. In recent years, the analysis of carbonate microfacies from petrology and sedimentology restores the original sedimentary background, and the establishment of a high-precision sedimentary facies evolution model and their controlling effect on the characteristics of reservoir space is one of the focuses of current research on favorable reservoirs in carbonate rocks [2–6]. The Ordovician Yingshan Formation has been considered an important carbonate reservoir in the

Tazhong area of the Tarim Basin. Studies on the sedimentary environment, facies distribution, and reservoir characteristics have intensified over the past decade [6–9]. However, detailed studies of the variation and associations of the microfacies on the Yingshan Formation are lacking, and the relationship between microfacies and reservoir space characteristics has not been thoroughly revealed on the same scale. Using a large number of research data such as core, thin section, logging data, imaging logging data (FMI), and field outcrop, based on the analysis of the microfacies, the paper tries to clarify the type of the carbonate microfacies and characteristics of reservoir space, thus providing a basis for the study of the evolution model of carbonate sedimentary environment and their constraint of favorable reservoirs in this area.

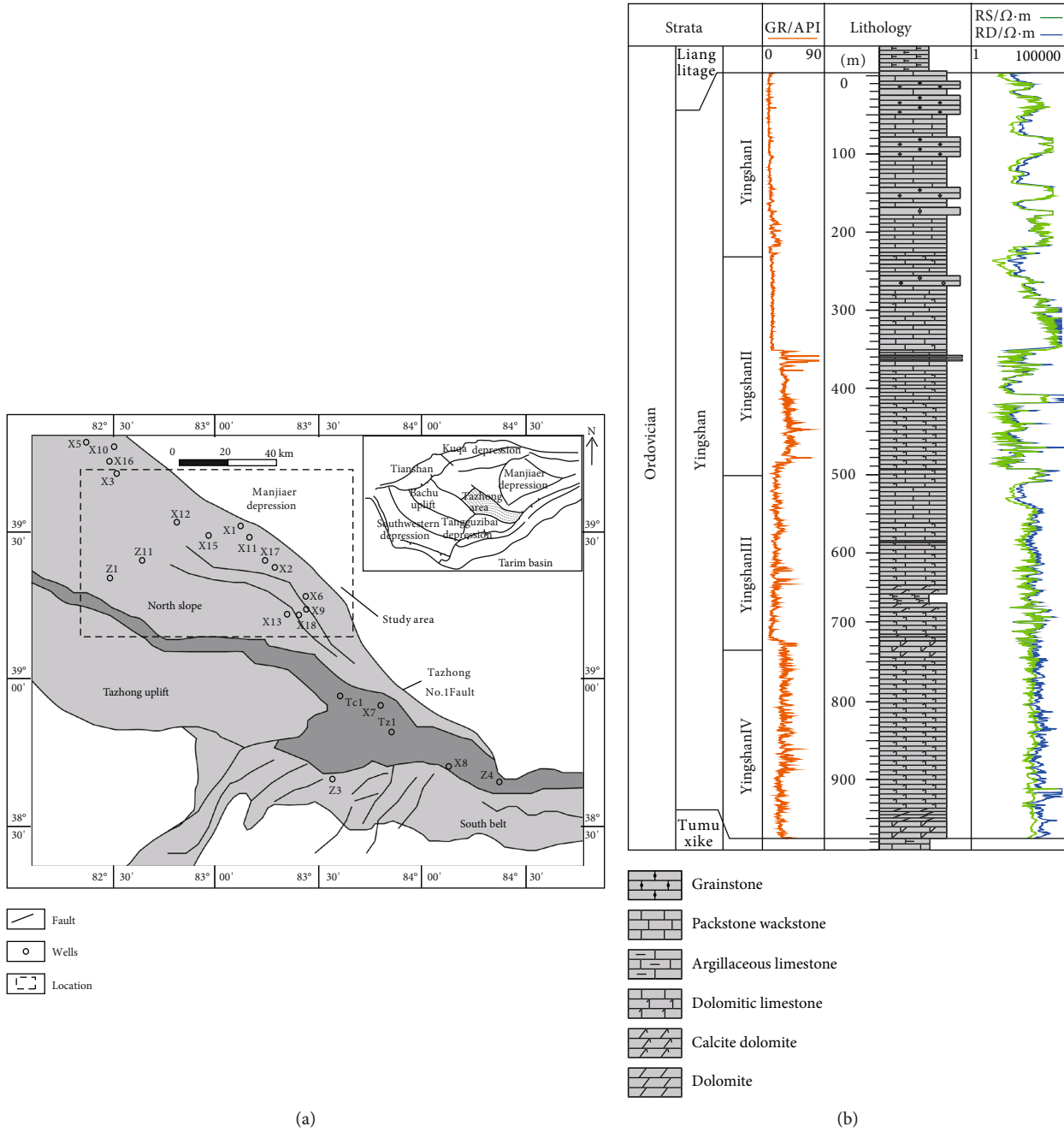


FIGURE 1: The tectonic location of Tazhong area (a) and composite stratigraphic section of the Yingshan Formation (b).

2. Geological Setting and Stratigraphic Characteristics

The Tazhong area is located in the middle of the central uplift belt, which spans the middle of the Tarim Basin in the east-west direction (Figure 1(a)). The research area is located in the slope zone north of the central fault zone of the Tazhong area, bordered by the Manjiaer sag to the east and connected to the central fault zone to the west [10, 11]. The research area has undergone a series of tectonic movements, forming complex geomorphological patterns. In the early days of the Caledonian movement, the basin remained under the background of continuous tension,

forming a series of tension faults, which lasted until the early Ordovician, during which large sets of carbonate platform deposits were developed in the Lower Ordovician Yingshan Formation. In the middle of the Caledonian movement, the Tazhong belt was denuded by uplift and developed large-scale angular unconformity, resulting in a large-scale deletion of the upper Yingshan Formation and the Tumuxiuke Formation in the Tazhong area. It was not until the early Late Ordovician period that it began to redeposit the Lianglitage Formation, with which was unconformated at an angle [12–14].

The Yingshan Formation can be divided into four sections from Yingshan I to Yingshan IV, with a total original

TABLE 1: Microfacies and sedimentary interpretation of Yingshan Formation.

Code	Microfacies	Description
Mf1	Oolitic grainstone	Grains are ooids of about 0.4 mm in size. The ooids underwent intense alteration, with the internal retained core clearly visible, while the laminated shell underwent dissolution and was filled with calcite (Figure 2(a)).
Mf2	Intraclast grainstone	Grains are mainly sand-sized intraclasts with amounts of algal spherical, which are better sorted and more uniform in size. And a very small amount of fine spherical mortar is filled in the middle (Figure 2(b)).
Mf3	Bioclastic grainstone	Most of grains in the rock are bioclastic with relatively large individuals, and the substrate is a granular colloid of sparry calcite (Figure 2(c)).
Mf4	Bioclastic intraclast grainstone	Internal debris particles range from 0.1 to 0.35 mm, with some grinding rounding, and the particles consist of mud crystal calcite with >70% content (Figure 2(d)).
Mf5	Peloid packstone	Peloids are the most abundant components, generally dominated by bright crystal cementation. The spherical particles are 0.1 mm in diameter, fine and uniform in size, mainly as tiny rounded mud crystal fragments (Figure 2(e)).
Mf6	Bioclastic wackestone	Most grains are silt-sized intraclasts, peloids, and bioclasts, including ostracodes, bryozoans, and algae (Figure 2(f)).
Mf7	Boundstone	Blue algae boundstone, wackestone, and mudstone with a laminar and bounded structure. Fenestral pores are common (Figure 2(g)).
Mf8	Mudstone	The rocks are mainly composed of microcrystalline calcite with a few siliceous particles, thin-bedded structure (Figure 2(h)).
Mf9	Micritic dolostone	This microfacies mainly consists of fine dolomite, basically no internal particles or raw chips inside (Figure 2(i)).

thickness of 800~1000 m [6, 15], which suffered strong denudation at a later stage, and the existing thickness is about 200~800 m, and the residual thickness varies greatly in different parts of the Tazhong area (Figure 1(b)). As a whole, the Yingshan Formation shows a transition process from calcite dolomite, dolomitic limestone, limestone to grainstone, and the calcium carbonate content gradually increases upward. The Yingshan IV Formation mainly develops dolomitic limestone, dolomite, dolomitic mudstone, and mudstone. The Yingshan III Formation is mainly dolomitic limestone, dolomitic limestone, and mudstone. The Yingshan II Formation is often subdivided into two subsections: the lower section of Yingshan II Formation is dominated by mudstone, wackestone, grainstone, dolomitic limestone, and calcite dolomite, and the upper section of Yingshan II is dominated by packstone, grainstone, and mudstone. And relatively dense mudstone and wackestone are mostly developed at the top. The Yingshan I Formation is subdivided into two subsections: the lower section of Yingshan I is dominated by mudstone and wackestone, and upper section is dominated by grainstone, packstone, and wackestone.

3. Microfacies and Microfacies Associations

The microfacies types of carbonate rocks identify the paleo-environment and sedimentary background by describing rock characteristics and paleontological characteristics. Carbonate microfacies analysis, particularly Dunham's carbonate petrological classification method [16], can provide information about the sedimentary environment and the evolution of different sedimentary microfacies, which can better explain the evolution of sedimentary paleo-environment in the study area [2]. Based on the identifica-

tion and analysis of nearly 400 thin sections from more than 20 wells, nine microfacies (Table 1) and four sedimentary microfacies associations in the study area were identified using Dunham's method.

Four types of microfacies associations (MA1–MA4) were identified based on microfacies stacking patterns that reflect correlative environments; each association represents a distinct facies succession (Figure 3). MA1 is platform interior intermediate- to high-energy bank, which includes several microfacies that were deposited in moderate- to high-energy background. This microfacies association is mainly developed in the upper part of the Yingshan I, the thickness is generally developed between 20 and ~50 m, the bottom is bioclastic wackestone (Mf6), and the middle is peloid packstone (Mf5) or bioclastic intraclast packstone. The succeeded bioclastic intraclast grainstone (Mf4) and bioclastic intraclast grainstone were generated in a subtidal photic zone with moderate to high wave energy and oolitic grainstone at the top of this microfacies associations (Mf1), or the relatively homogeneously sorted intraclast grainstone (Mf2), with exposed structures sometimes. MA1 forms a set of upwardly shallowing sedimentary cycle reflecting a relatively high- to moderate-energy condition with relatively large thickness and lateral ductility.

MA2 is platform interior low-energy bank, which is widely developed in the study area, with thicknesses ranging from 20 to 50 m. The bottom part is mudstone (Mf8), and the upper part is bioclastic intraclast grainstone (Mf4) or peloid packstone (Mf5), and the top part is mainly intraclast grainstone (Mf2) or bioclastic grainstone (Mf3), interspersed with thin layers of bioclastic wackestone (Mf6). This microfacies associations also reflects an upwardly shallowing sedimentary cycle; the sedimentary environment energy is increasing shift.

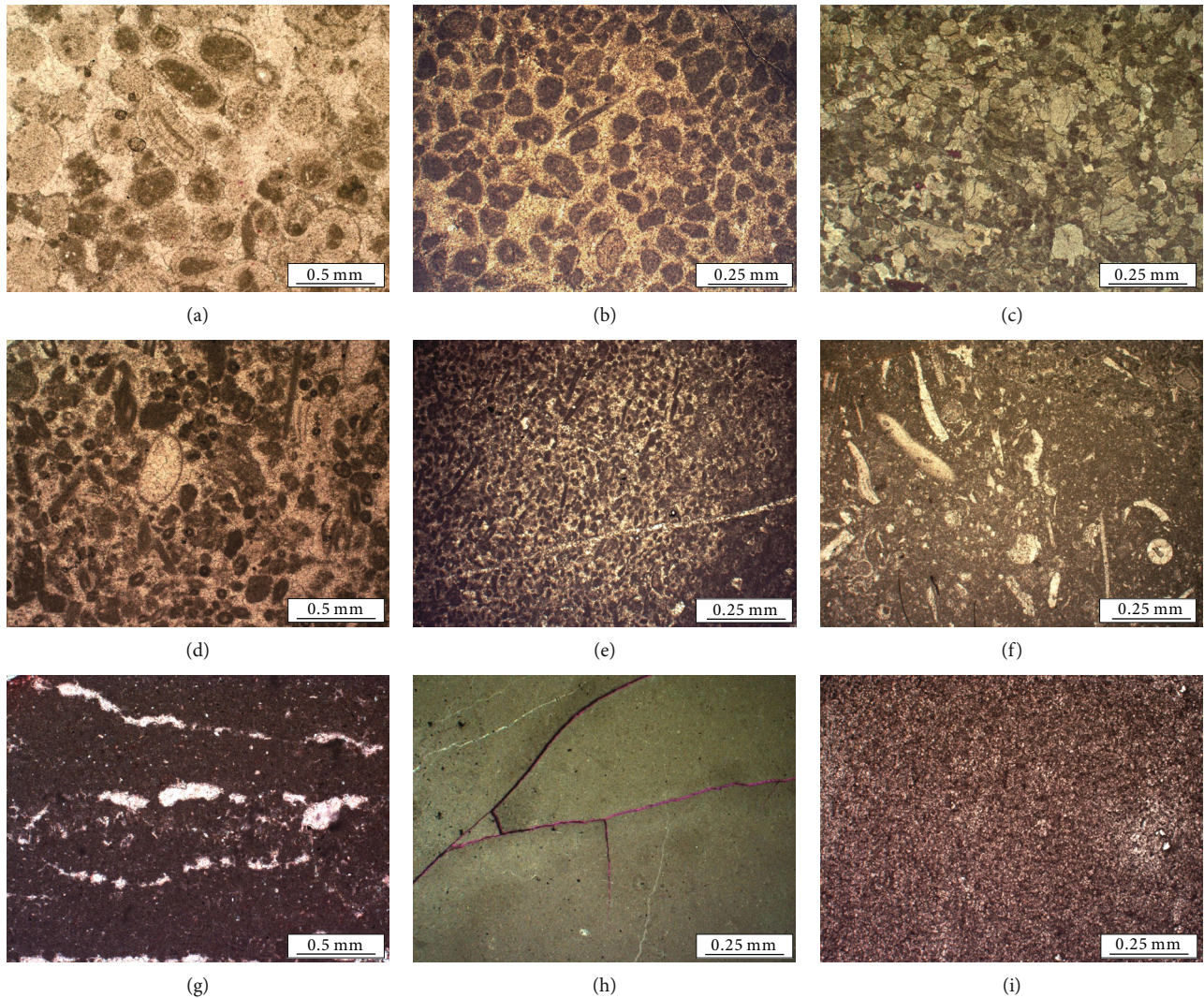


FIGURE 2: Main microfacies of Yingshan Formation in Tazhong area (Mf1-Mf9). (a) Mf1, oolitic grainstone, X3 well, 6650 m. (b) Mf2, intraclast grainstone, X171. (c) Mf3, bioclastic grainstone, X16, 6417.54 m. (d) Mf4, bioclastic intraclast grainstone, X452, 6370.53 m. (e) Mf5, peloid packstone, X9, 6247.79 m. (f) Mf6, bioclastic wackestone, X452, 6370.53 m. (g) Mf7, bioclastic wackestone, X5, 6285 m. (h) Mf8, mudstone, X41, 5540.85 m, x25. (i) Mf9, microcrystal dolomite, X512, 5589 m.

MA3 is platform interior tidal flat, which was developed in the Yingshan II, with thicknesses ranging from 20 to 40 m. Mudstone (Mf8) and sometimes bioclastic wackestone (Mf6) are developed at the bottom, peloid packstone (Mf5) or bioclastic wackestone (Mf6) at the middle, boundstone (Mf7) upwards, and mudstone (Mf8) at the top. It reflects the microfacies association developed in the tidal environment of interior platform.

MA4 is platform interior tidal flat and intrabank sea, which includes several microfacies that are generated in a relatively low- to moderate-energy condition, indicating restricted lagoons and tidal flat environments. MA4 is mainly developed in the lower part of Yingshan III and Yingshan IV, occasionally in Yingshan II, and the thickness is generally in the range of 10~30 m, and the top is mainly developed as microcrystal dolomite and dolomitic mudstone interbedded (Mf9). The vertical stacking pattern of these microfacies reflects the change in depositional setting from

a subtidal lagoonal environment to an intertidal and to a supratidal environment on the platform interior.

4. Characteristics of Reservoir Space in the Yingshan Formation

The Lower-Middle Ordovician Yingshan Formation mainly went through the Middle Caledonian-Early Hercynian tectonic movements. And the influence of multiple phases of tectonic activity occurred in the later stages, which led to the development of multigenetic dissolution pores and fractures within it [8, 17, 18].

Based on the observation of microscopic thin sections, core description, and logging data, especially combined with the microresistivity imaging logging data (FMI), the reservoir space within the Yingshan Formation can be finely analyzed and identified [19, 20], and it is classified into four types of reservoir space: small dissolution pore type,

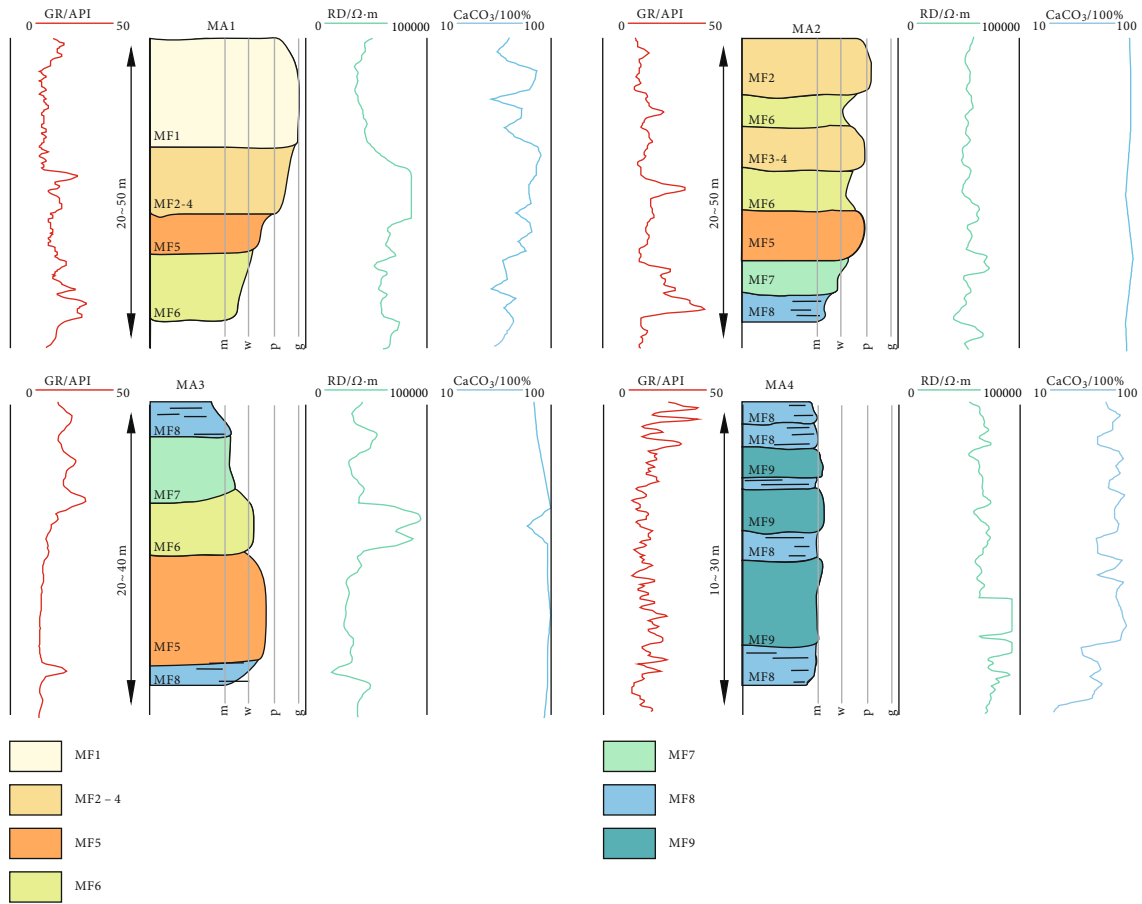


FIGURE 3: Microfacies associations pattern in Yingshan Formation (MA1-MA4).

fracture-dissolution pore type, fracture type, and large-scale karst-cavity type.

The reservoir spaces of small dissolution vug type can be divided into several categories under the microscope, including primary fabric-selective pores, such as intergranular pores (Figure 4(a)), melodic pores, and biological cavity pore (Figure 4(b)), and fenestral structures (Figure 4(c)) mostly filled by calcite. It also includes small dissolution (Figure 4(d)) and dolomite intergranular pores (Figure 4(e)) formed by buried karst at a later stage, among which the grainstone intergranular pores and dolomite intergranular pores are the ones that contribute most to the reservoir space, with porosity up to 10% or more. Pores of different sizes can also be observed in the cores, and some of them can be seen to be obviously developed along the layer. Small dissolution vugs of multiple geneses show a large number of obvious paralleling or honeycomb dark spots on FMI imaging logs, mainly in clusters or strips, which are easily distinguished from the high-resistance bright-colored enclosing rocks (Figure 5(a)).

Fracture-dissolution pore reservoir space consists of two parts: fractures and small dissolution vugs. The fractures are mainly developed into structural fractures, dissolution fractures, and diagenetic shrinkage fractures. The type and origin of internal dissolution pores are basically the same as those of small dissolution vug reservoir spaces, the difference is that the porosity and permeability of the reservoir are

improved due to the communication between fractures and dissolution pores in this type of reservoir space. It is the most favorable reservoir space in the Yingshan Formation.

The fracture-dissolution pore reservoir space also appears as dark bands or honeycomb-like dark spots on imaging logging, with a large number of dark high-conductivity fractures developed inside, and dark pores are often distributed along the open fractures in the form of beads or veins (Figure 5(b)).

Structural fractures and dissolution fractures are widely developed in the Yingshan Formation, among which structural fractures are dominated, mostly high-angle fractures and middle- to high-angle fractures. It can be seen that multistage fractures cut each other, and these fractures are cut and connected to each other to form a fracture-type reservoir space (Figure 4(f)). Dissolution fractures are mainly formed by pressure solution, which belongs to chemical dissolution. Dissolution develops near the fractures, and the interior is sometimes filled with mud or calcite, while the dissolution pores are underdeveloped, and the thickness and linear density of fractures in different well sections are various. It is linearly distributed on imaging logging and presents a network-like feature as the fracture density gradually increases [21] (Figure 5(c)).

The large-scale karst-cavity reservoir space (Figure 5(d)) mostly refers to the karst caves with a diameter of more than 10 cm. The scale of karst caves developed in the Yingshan

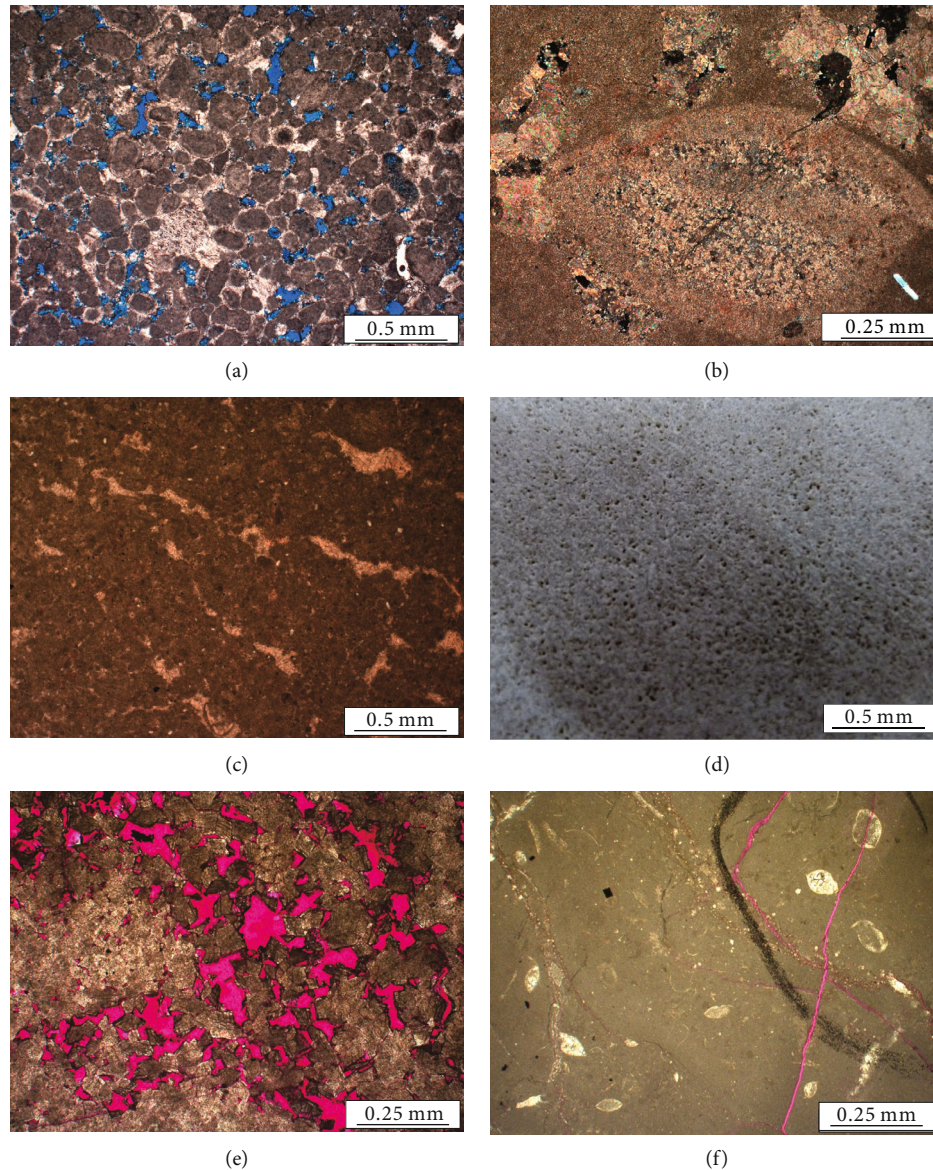


FIGURE 4: Reservoir space of Yingshan Formation. (a) X203 well, 6581.72 m. (b) X7 well, 5800 m. (c) X7 well, 5965.5 m. (d) X203 well, 6567.38 m~6573.38 m. (e) X9 well, 6265.01 m. (f) X41 well, 5542.7 m.

Formation ranges from tens of centimeters to several meters, and the larger ones can reach more than ten meters.

Through imaging logging, it can be observed that its interior is often filled or semifilled with collapsed breccia, thin mudstone, etc. Collapsed boulders are often mixed in size, with particle sizes ranging from several centimeters to several meters. Mud often deposits on the top of the cave or inside the cave, filled with thin-layered calcareous mudstone and sandy mudstone, and sometimes horizontal laminae can be developed. Based on the statistics of more than 20 wells in the Tazhong area, the thickness of various types of reservoir spaces is calculated, among which fracture-dissolution pore type accounts for 56.90%, small dissolution vug type accounts for 24.60%, and fracture-type and large-scale karst-cavity type each account for 10.10% and 8.40%.

It can be seen that the fracture-dissolution pore-type reservoir space is the most important reservoir space in the Yingshan Formation, followed by the small dissolution vug

type, while the proportion of fracture type and karst-cavity type is relatively small.

5. Relationship between Microfacies and Characteristics of Reservoir Space in Yingshan Formation

According to recent research, carbonate reservoirs are controlled by many factors, including supergene karst, hydrothermal process, and tectonic movement [22, 23]. But microfacies are the material basis and prerequisites for carbonate reservoirs, which control the texture and lithology of rocks, thus controlling the development of primary pores in carbonate rocks and affecting the development of dissolved pores to a large extent. The geological understanding of reservoir genesis and characteristics may provide an

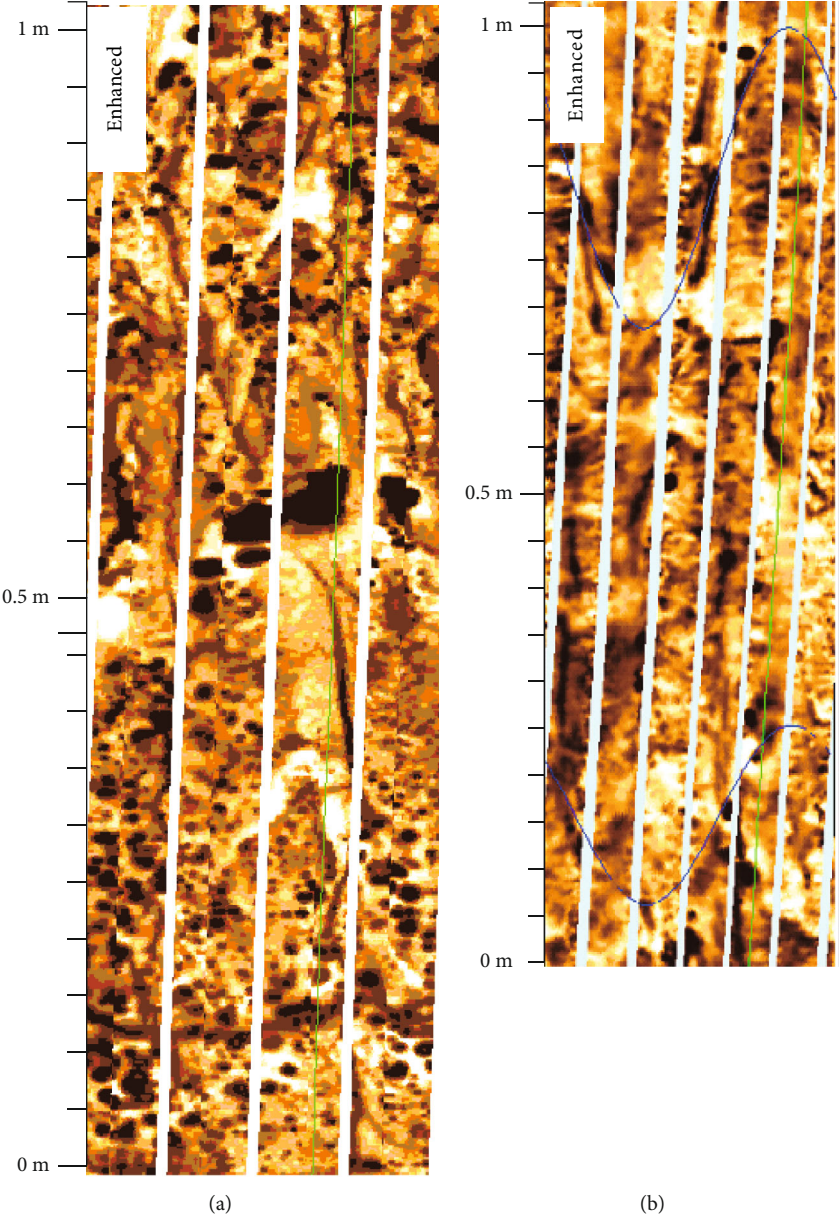


FIGURE 5: Continued.

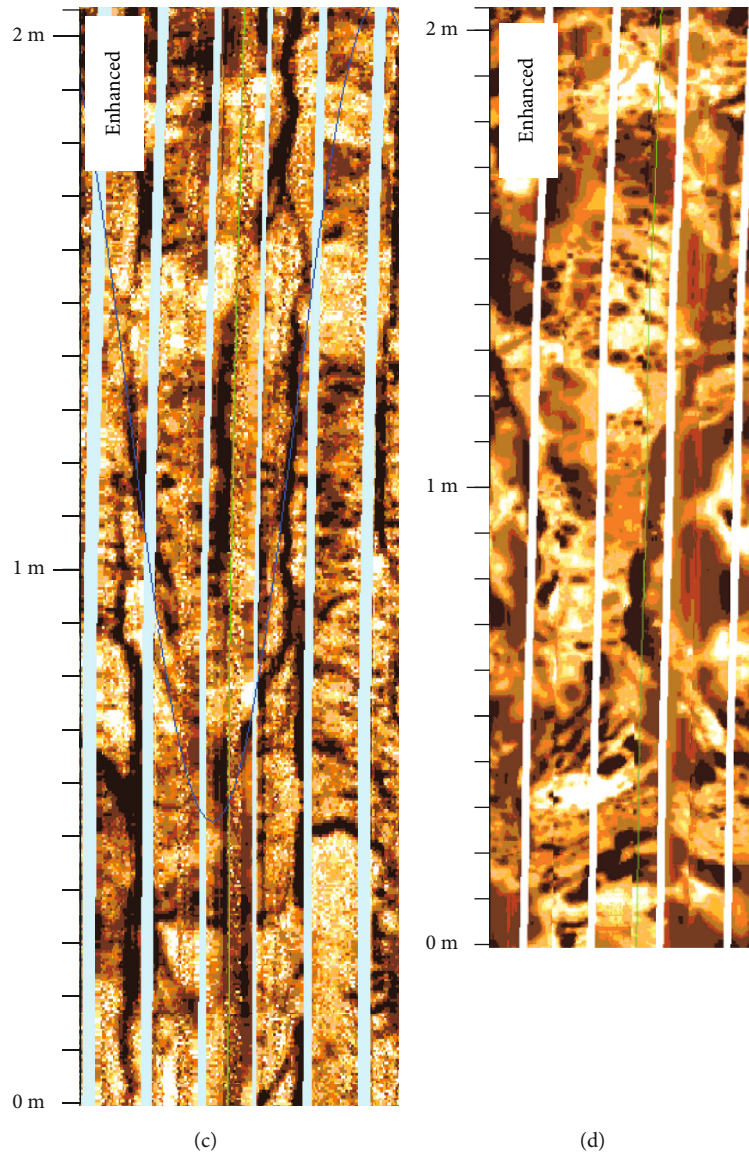


FIGURE 5: FMI interpretation of carbonate reservoir space.

important reference for seeking potential favorable carbonate reservoirs on Yingshan Formation. The development of carbonate microfacies is very sensitive to the rise and fall of sea level and often has a rapid response to its changes [24–26]. The development of different sedimentary microfacies sequences has different effects on the development of favorable reservoirs (Figure 6). According to the analysis of carbonate microfacies from multiple wells in the study area, there are microfacies associations developed in each layer of the Yingshan Formation, and these associations have a certain continuity in the lateral direction. The wave energy of the sedimentary microfacies at the bottom is relatively weak and gradually strengthened upward. At the same time, by identifying the reservoir space type of each well, it can be seen that the distribution pattern of sedimentary microfacies affects the development of favorable reservoirs in the later stage.

The MA1 and MA2 tend to develop small dissolution pore-type reservoir spaces and fracture-type reservoir spaces, especially in oolitic grainstone (Mf1) and intraclast grainstone (Mf2), which exist in the form of intergranular pores, intragranular pores, and mold pores, while bioclastic grainstone (Mf3) mainly develops intergranular pores and intragranular pores. At the same time, MA1-MA2 are prone to forming structural fractures due to changes in structure and stress. These fractures are connected to the pores formed by multitemporal and multifactors [7], which further improves the physical properties of the reservoir in the Yingshan Formation.

These high-energy wave microfacies developed at the top of the sequence are easily affected by the upper unconformity to form large-scale karst-cavity reservoir spaces [27]. At the same time, MA3 and MA4 which are formed in the low-energy background mostly appear in the form of

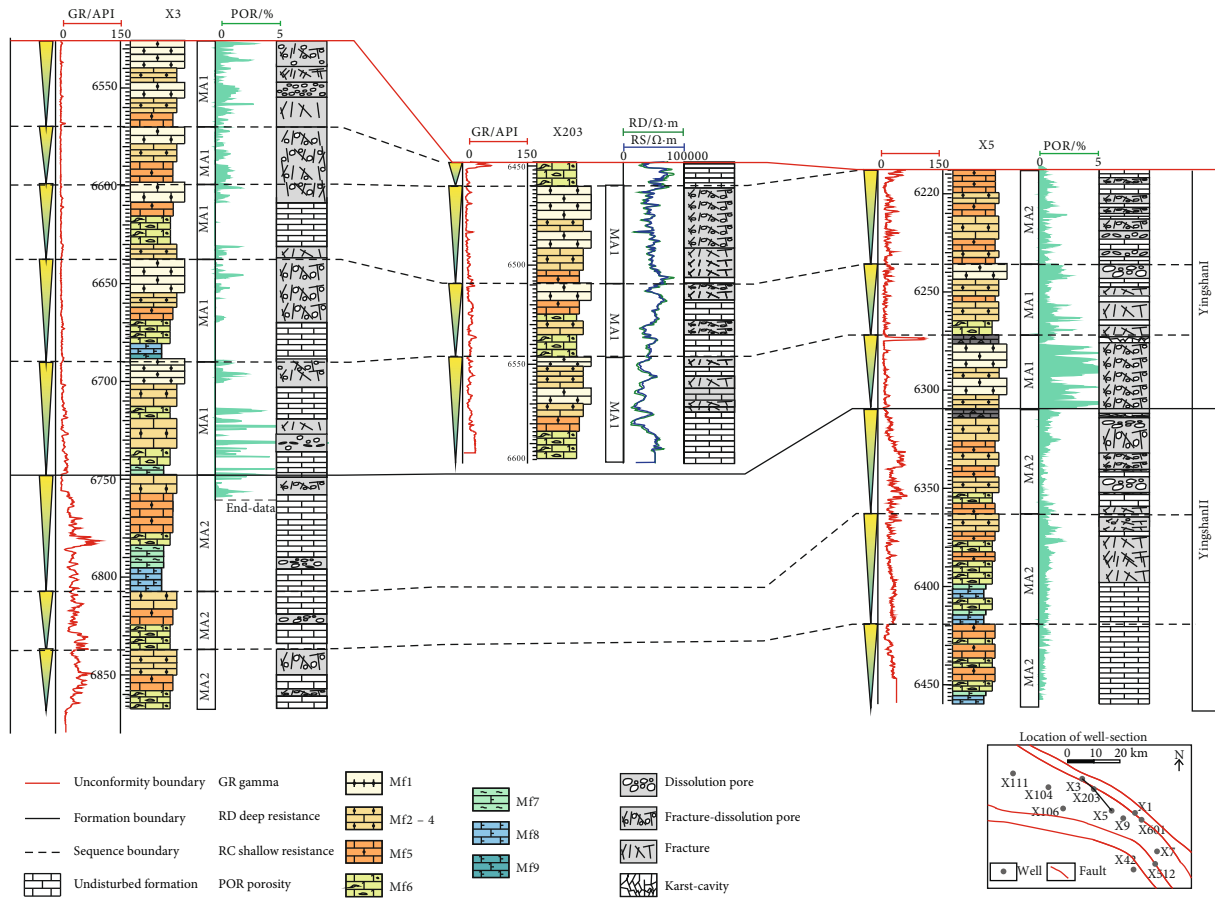


FIGURE 6: Microfacies association and reservoir space correlation section in Tazhong area.

undisturbed strata or interlayers that are not easily transformed or dissolved. Sometimes, they will develop fractured reservoir spaces or a small amount of fracture-dissolution pore reservoirs due to superimposed reformation.

6. Conclusion

- (1) Nine microfacies (Mf1-Mf9) and four microfacies associations (MA1-MA4) were identified within the Ordovician Yingshan Formation. MA1-MA2 represent a medium- to high-energy sedimentary background and MA3-MA4 represent a medium- to low-energy sedimentary background; each association represents a distinct facies succession
- (2) Through the data of thin sections, cores, imaging logging, and other data, four kinds of reservoir spaces can be identified: small dissolution vug type, fracture-dissolution pore type, fracture type, and large-scale karst-cavity type in the Yingshan Formation. Fracture-dissolution pore type is the most important reservoir space in the Yingshan Formation, followed by small dissolution vug type, while fracture type and large-scale karst-cavity type account for a relatively small proportion

- (3) The high-energy microfacies associations (MA1-MA2) are more developed with small dissolution vug type reservoir space and fracture-dissolution pore-type reservoir space. Internal pores and fractures are superimposed to form high-quality reservoirs in the Yingshan Formation. Sometimes in the high part of the sequence, large karst caves filled with argillaceous can be observed. The low-energy sedimentary microfacies associations (MA3-MA4) mostly appear in the form of undisturbed formations or interlayers. However, due to tectonic movement and superimposed transformation of buried karst, a small amount of fractured and fracture-dissolution pore-type reservoir spaces will develop in a few locations

Data Availability

All data are in the paper.

Conflicts of Interest

The author declares that there is no conflict of interest regarding the publication of this paper.

Acknowledgments

This work was supported by the National Key R&D Program Project of China “Genesis of Subsalt Ultra-Deep Carbonate Reservoirs and Hydrocarbon Accumulation Mechanism” (Grant No. 2019YFC0605502), National Natural Science Foundation of China (Grant No. 42230816), and the Major Scientific and Technological Projects of CNPC (Grant No. ZD2019-183-002).

References

- [1] X. Y. Yang, J. X. Fan, Y. Zhang, W. H. Li, Y. Du, and R. Yang, “Microscopic pore structure characteristics of tight limestone reservoirs: new insights from section 1 of the Permian Maokou formation, southeastern Sichuan basin, China,” *Unconventional Resources*, vol. 2, pp. 31–40, 2022.
- [2] E. Flügel, *Microfacies of carbonate rocks analysis interpretation and application*, Springer, Germany, 2004.
- [3] D. Gao, C. S. Lin, H. J. Yang et al., “Microfacies of Late Ordovician Lianglitage formation and their control on favorable reservoir in Tazhong area,” *Earth Science—Journal of China University of Geosciences*, vol. 38, no. 4, pp. 819–831, 2013.
- [4] D. Gao, C. S. Lin, H. J. Yang et al., “Microfacies and depositional environments of the Late Ordovician Lianglitage formation at the Tazhong uplift in the Tarim basin of Northwest China,” *Journal of Asian Earth Sciences*, vol. 83, no. APR.1, pp. 1–12, 2014.
- [5] J. Q. Liu, Z. Li, J. C. Huang, Y. X. Han, H. J. Peng, and Z. Zhong Cai, “Distinct sedimentary environments and their influences on carbonate reservoir evolution of the Lianglitag formation in the Tarim basin, Northwest China,” *Science China: Earth Sciences*, vol. 55, no. 10, pp. 1641–1655, 2012.
- [6] C. H. Sun, H. J. Yang, W. Q. Pan et al., “Fine division of Yingshan formation of Ordovician in Tazhong area, Tarim basin,” *Xinjiang Petroleum Geology*, vol. 33, no. 1, pp. 46–48, 2012.
- [7] W. Liu, X. Y. Zhang, and H. Y. Gu, “Sedimentary environment of lower-middle Ordovician Yingshan formation in mid-western Tarim basin,” *Acta Sedimentologica Sinica*, vol. 27, no. 3, pp. 435–442, 2009.
- [8] Y. X. Qian, X. G. Sha, H. L. Li et al., “An approach to Caledonian unconformities and sequence stratigraphic patterns and distribution of reservoirs of Ordovician carbonate in the western Tazhong area, Tarim basin,” *Earth Science Frontier*, vol. 20, no. 1, p. 260, 2013.
- [9] P. Ren, C. S. Lin, J. F. Han, H. Li, J. Y. Liu, and Q. L. Wang, “Microfacies characteristics and depositional evolution of the Lower Ordovician Yingshan formation in northslope of Tazhong area, Tarim basin,” *Natural Gas Geoscience*, vol. 26, no. 2, pp. 241–254, 2015.
- [10] C. S. Lin, H. J. Yang, J. Y. Liu et al., “Tectonic geomorphology of the Paleozoic central uplift belt and its constraint on the development of depositional facies in the Tarim basin,” *China Science*, vol. 39, no. 3, pp. 306–316, 2009.
- [11] C. S. Lin, S. T. Li, J. Y. Liu et al., “Tectonic framework and paleogeographic evolution of the Tarim basin during the Paleozoic major evolutionary stages,” *Acta Petrologica Sinica*, vol. 27, no. 1, pp. 210–218, 2011.
- [12] D. Gao, C. S. Lin, M. Y. Hu, H. J. Yang, and L. L. Huang, “Paleokarst of the Lianglitage formation related to tectonic unconformity at the top of the Ordovician in the eastern Tazhong uplift, Tarim basin, NW China,” *Geological Journal*, vol. 53, no. 2, pp. 458–474, 2018.
- [13] C. S. Lin, H. J. Yang, J. Y. Liu et al., “Sequence architecture and depositional evolution of the Ordovician carbonate platform margins in the Tarim basin and its response to tectonism and sea-level change,” *Basin Research*, vol. 24, no. 5, pp. 559–582, 2012.
- [14] C. S. Lin, H. J. Yang, J. Y. Liu, Z. F. Rui, Z. Z. Cai, and Y. F. Zhu, “Distribution and erosion of the Paleozoic tectonic unconformities in the Tarim basin, Northwest China: significance for the evolution of paleo-uplifts and tectonic geography during deformation,” *Journal of Asian Earth Sciences*, vol. 46, pp. 1–19, 2012.
- [15] H. F. Yu, Z. K. Bai, L. P. Deng, W. W. Jiao, Y. Y. Pan, and Y. Zhao, “Determination and geologic significance of Yingshan unconformity of Lower Ordovician in Tazhong area, Tarim basin,” *Xinjiang Petroleum Geology*, vol. 32, no. 3, pp. 231–234, 2011.
- [16] R. J. Dunham, “Classification of carbonate rocks according to their depositional texture,” in *Classification of carbonate rocks*, W. E. Ham, Ed., A symposium: AAPG memoir, 1962.
- [17] G. Y. Zhang, W. Liu, L. Zhang et al., “Cambrian-Ordovician prototypic basin, paleogeography and petroleum of Tarim craton,” *Earth Science Frontiers*, vol. 22, no. 3, pp. 269–276, 2015.
- [18] Z. J. Zhao, “Indicators of global sea-level change and research methods of marine tectonic sequences: take Ordovician of Tarim basin as an example,” *Acta Petrolei Sinica*, vol. 36, no. 3, pp. 262–273, 2015.
- [19] Z. W. Luo, R. C. Xie, W. L. Cai, Y. F. Wang, M. Z. Deng, and Y. Feng, “Comprehensive logging identification method of shell limestone fractures in the Lower Jurassic Da’anzhai member in the Dongpo area of the Western Sichuan depression,” *Unconventional Resources*, vol. 2, pp. 97–107, 2022.
- [20] G. F. Zhong and Z. T. Ma, “Sedimentary structures identified from high-resolution borehole micro-resistivity image logs,” *Journal Of Tongji University*, vol. 29, no. 5, pp. 576–580, 2001.
- [21] W. Q. Pan, G. T. Hou, Y. M. Qi, P. Zhang, Y. Q. Chen, and W. Ju, “Discussion on the development models of structural fractures in the carbonate rock,” *Earth Science Frontiers*, vol. 20, no. 5, pp. 188–195, 2013.
- [22] H. H. Chen, Z. Y. Lu, Z. C. Cao, J. Han, and L. Yun, “Hydrothermal alteration of Ordovician reservoir in northeastern slope of Tazhong uplift, Tarim basin,” *Acta Petrolei Sinica*, vol. 37, no. 1, pp. 43–63, 2016.
- [23] W. Z. Zhao, A. J. Shen, W. Q. Pan, B. M. Zhang, Z. F. Qiao, and J. F. Zheng, “A research on carbonate karst reservoirs classification and its implication on hydrocarbon exploration: cases studies from Tarim basin,” *Acta Petrologica Sinica*, vol. 29, no. 9, pp. 3213–3222, 2013.
- [24] D. Gao, M. Y. Hu, A. P. Li, W. Yang, W. R. Xie, and C. Y. Sun, “High-frequency sequence and microfacies and their impacts on favorable reservoir of Longwangmiao formation in Central Sichuan basin,” *Earth Science*, vol. 46, no. 10, pp. 3520–3534, 2021.
- [25] D. Gao, M. M. Wang, Y. Tao, C. Y. Sun, X. M. Huang, and J. W. Wu, “Control of sea level changes on high-frequency sequence and sedimentary evolution of Lianglitage formation in the Tazhong Area,” *Geology in China*, vol. 49, no. 6, pp. 1936–1950, 2022.

- [26] Y. R. Zhao, D. Gao, M. Y. Hu, C. Zheng, J. Li, and W. R. Xie, "Controls of paleoclimate and sea-level changes on the high-frequency sequence of shallow-water carbonates: a case study of the Longwangmiao formation in the central Sichuan basin," *Geology in China*, 2022.
- [27] Z. S. Ke, B. Feng, Y. G. Liu, Z. P. Cui, and X. Y. Liu, "Dissolution and sedimentation patterns of typical minerals in artificial reservoirs under different environments," *Unconventional Resources*, vol. 2, pp. 60–71, 2022.